



Functional Imaging of the Liver

Simona Picchia, Martina Pezzullo,
Maria Antonietta Bali, Septian Hartono,
Choon Hua Thng, and Dow-Mu Koh

Contents

1	Introduction	396
2	Functional Imaging Techniques in the Liver	396
3	Assessing Liver Perfusion	398
3.1	Background Considerations	398
3.2	Computed Tomography Perfusion Imaging	398
3.3	Dynamic Contrast-Enhanced MR Imaging (DCE-MRI)	401
4	Assessing Cellularity and Microstructural Organisation	404
4.1	Background Considerations	404
4.2	Clinical Applications	404
5	Assessing Tissue Elasticity and Stiffness	407
5.1	Background Consideration	407
5.2	Clinical Applications	408
6	Evaluation of Liver Function	409
6.1	Background	409
6.2	Clinical Application	409
7	Future Developments	410
	References	412

S. Picchia
Department of Radiology, University “La Sapienza”,
Rome, Italy

M. Pezzullo
Department of Radiology, Erasme Hospital,
Université Libre de Bruxelles, Brussels, Belgium

M. A. Bali
Department of Radiology, Institut Jules Bordet,
Université Libre de Bruxelles, Brussels, Belgium

S. Hartono · C. H. Thng
Department of Diagnostic Imaging, National Cancer
Centre, Singapore, Singapore

D.-M. Koh (✉)
Department of Radiology, Royal Marsden Hospital,
London, UK
e-mail: dowmukoh@icr.ac.uk

Abstract

Traditionally, imaging of focal and diffuse liver diseases has relied on morphological assessment on ultrasound, CT and MRI. However, morphological changes detectable on conventional imaging may be insensitive to early disease or therapeutic effects. For this reason, functional imaging techniques are increasingly used to evaluate liver diseases. The most widely investigated functional measurements include perfusion imaging (CT and MRI), diffusion-weighted MRI, MR elastography and quantitative T1-weighted gadoxetate-enhanced MRI of the liver. These techniques are used to improve disease detection, assess therapeutic effects and also evaluate liver function. The technical implementation, clinical utility and evidence for their deployment are discussed in this chapter.

1 Introduction

The liver is a large, richly vascularised, solid organ that is easily accessible to various imaging modalities such as ultrasonography (US), computed tomography (CT), magnetic resonance (MR) and positron emission tomography (PET) for detection, characterisation and monitoring of diffuse and focal hepatic diseases. Morphological imaging remains the cornerstone for radiological assessment of the liver, although functional imaging techniques are being increasingly deployed. Functional imaging techniques can reflect liver pathophysiology and allows quantitative measurements to be made, which are used to quantify changes associated with disease states. Studies have shown that functional imaging techniques can aid early disease detection, characterise disease behaviour, provide an early assessment of therapeutic effects or yield insights into disease prognosis.

In this chapter, we survey the functional imaging techniques that can be applied towards the assessment of both focal and diffuse liver diseases. A comprehensive survey of all functional liver imaging techniques is beyond the scope of

this chapter. Hence, we focus our discussion on the use of functional imaging to study liver perfusion, tissue cellularity and microstructural organisation, liver stiffness and hepatocyte function. The clinical utility and limitations of these techniques is discussed, together with the evolving developments in the field.

2 Functional Imaging Techniques in the Liver

Functional CT, MRI and molecular imaging techniques can be applied to evaluate the liver. The most widely investigated functional CT technique is perfusion CT, which requires rapid and repeated scanning of the liver following intravenous contrast administration. This allows parameters that reflect blood flow in the liver to be derived. As CT perfusion studies can result in significant radiation burden, its adoption has been limited to clinical trials and specialised centres. Some investigators regard the use of dual-energy CT image acquisition as a functional imaging technique, as data acquired using x-rays of different energies can be used to derive quantitative information, such as tissue iodine concentration following intravenous contrast injection, which is linked to tissue perfusion.

MRI is the most versatile functional liver technique for the liver, as different image acquisition techniques can be used to derive specific measurement parameters, each reflecting a different aspect of liver pathophysiology. Using dynamic contrast-enhanced MRI, perfusion MRI is performed, which is used to characterise blood flow in liver tumours and their response to treatment. Intrinsic susceptibility MRI (IS-MRI) can provide insights into tumour blood volume and tissue oxygenation, although the technique is not often applied in the liver. By contrast, diffusion-weighted imaging (DWI) is now widely used in the liver to study tissue cellularity and microstructural organisation. In clinical practice, DWI is most often used to highlight cellular disease from the rest of the normal liver parenchyma, without the need for exogenous contrast administration. The use of DWI has significantly

enhanced the clinical diagnostic confidence for the detection of focal liver lesions and is a key sequence in emerging abbreviated liver imaging protocols, which aims to accelerate liver MR imaging without compromising diagnostic performance. MR elastography, which is used to measure liver stiffness, is a useful technique to assess for liver fibrosis and cirrhosis. The adoption of MR elastography requires hardware investment, which means that it is not often available beyond specialist liver centres, where there is a significant caseload to justify its deployment. More recently, there has been significant interest in the use of MRI to assess hepatic function. To achieve this, MR imaging is performed following the injection of a hepatocyte selective contrast medium, and temporal changes in the quantita-

tive T1 relaxation time is used to estimate the hepatocyte function.

For molecular imaging, the most widely used radiotracer remains as 18F-deoxyglucose (18F-FDG), which is widely used in the cancer setting to detect hypermetabolic tumours; and to monitor their response to treatment. However, other molecular tracers, such as Ga68-DOTATATE and 18F-choline, have also their utility in a specific context, the former for the assessment of neuroendocrine liver metastases; and the latter for the assessment of liver tumours (e.g. hepatocellular carcinoma). Further discussion of molecular imaging techniques for liver assessment is beyond the scope of this chapter. The commonly used functional imaging techniques used to assess the liver are summarised in Table 1.

Table 1 Functional imaging techniques for liver imaging

Imaging Technique	Biological correlates	Examples of measurement parameters
CT		
Perfusion CT	Blood flow, vascular permeability, microvessel density	Non-quantitative: Shape of the enhancement curve Semi-quantitative: Hepatic perfusion index, time to peak, slope of enhancement, area under the curve Quantitative: Blood flow, vascular permeability, relative hepatic artery and portal vein blood flow, extracellular volume
MRI		
Perfusion MRI	Blood flow, vascular permeability, microvessel density,	Non-quantitative: Shape of the enhancement curve Semi-quantitative: Hepatic perfusion index, time to peak, slope of enhancement Quantitative: Blood flow, vascular permeability, relative arterial and portal vein blood flow, extracellular volume
Intrinsic susceptibility MRI	Blood volume, tissue oxygenation	Blood volume, T2* relaxivity
Diffusion-weighted MRI	Tissue cellularity, extracellular space tortuosity, microstructural organisation, fluid viscosity	Monoexponential model: Apparent diffusion coefficient (ADC) Non-monoexponential models: Intravoxel incoherent motion: Perfusion fraction, pseudodiffusion coefficient, diffusion coefficient Diffusion kurtosis: Kurtosis, diffusion coefficient
MR elastography	Tissue stiffness, tissue elasticity	Shear stiffness
Fat and water quantification	Intravoxel fat and iron	Percentage of fat and iron in the liver
Change in T1 relaxivity of the liver after hepatocyte selective contrast medium	Hepatocellular function	Change in T1 relaxation time, hepatocyte extraction ratio
Molecular imaging		
18F-FDG PET	Glucose metabolism	Standardised uptake values
18F-choline PET	Cellular membrane turnover	Standardised uptake values
68Ga-DOTATE PET	Expression of somatostatin receptor 2	Standardised uptake values

3 Assessing Liver Perfusion

3.1 Background Considerations

Imaging liver perfusion can be a challenging task because the liver has a unique dual vascular supply with approximately 25% of hepatic blood flow originating from the hepatic artery and 75% from the portal vein (Chiandussi et al. 1968). Both these afferent vascular systems communicate with each other through trans-sinusoidal and transvasal network and the peribiliary plexuses. The aim of perfusion imaging is to non-invasively obtain information on normal and pathologic hepatic microcirculation and to identify possible imaging biomarkers reflecting the underlying physiology/physiopathology that aids the detection and characterisation of pathological conditions and for predicting and monitoring response to treatment.

When primary tumours or metastatic deposits are present within the liver, they will lead to hemodynamic changes of the hepatic blood flow that can be detected by perfusion imaging. These changes are related to tumour neo-vascularisation which represents a key factor for tumour growth, progression and metastasis. Tumour neo-vascularisation is a complex process that is induced and mediated by tumour and host-related factors responsible for increased vessel density consisting of new non-endothelialised highly leaky capillaries and arteriovenous shunts (Dvorak et al. 1995; Lee et al. 2003). However, neo-vascularisation also means that tumours in the liver derive their blood supply predominantly from the hepatic artery rather than the portal vein. Tumours with high vascularity also show more aggressive behaviour and are associated with worse disease outcomes (Henderson et al. 2003).

Ideally, the following requirements should be considered when performing liver perfusion using imaging modalities: high temporal and spatial resolution images to correctly identify the kinetic properties of the tracer; accurate quantification of global or regional arterial and portal perfusion; calculation of tracer concentrations for an accurate quantitative study; robust modelling of liver perfusion physiology; and whole-liver coverage.

3.2 Computed Tomography Perfusion Imaging

The general principle of computed tomography perfusion imaging (CTPI) is based on monitoring changes of iodinated contrast agent concentration in the hepatic blood vessels and tissue as a function of time following intravenous injection. These contrast agent concentrations are linearly proportional to the CT attenuation changes within the vascular structures and the tissue expressed in Hounsfield units (Axel 1980). Therefore, temporal changes in attenuation can be analysed to provide several parameters that reflect the underlying vascular and tissue physiology/physiopathology.

The vascular and tissue attenuation curves versus time are obtained by placing a region of interest (ROI) respectively on the hepatic artery (or abdominal aorta), the portal vein and the tissue/lesion being analysed, on the dynamic CT images acquired with high temporal resolution (e.g. 1 image/sec for the first pass of contrast agent in the tissue) before, during and after the intravenous administration of an iodinated contrast agent using a power injector. In the presence of image misregistration, mainly due to respiratory motion, the use of motion correction tools is recommended (Miles et al. 2012). From these contrast concentration-time curves, CTPI parameters can be calculated using either a model-free or a model-based approach (Kim et al. 2014).

In the model-free approach, only the perfusion phase (first-pass of contrast material) is taken into account which allows calculation of the hepatic arterial and portal venous perfusion (PVP) and the hepatic perfusion index (HPI) (Miles et al. 1993). The model-based approach has moved towards a dual-input, dual compartment pharmacokinetic model, provided that there is good data support for such analysis. The dual-input model respects the dual vascular supply of the liver from the hepatic artery and the portal vein. However, when evaluating hepatic metastases or hepatocellular carcinoma (HCC), which are known to be predominantly supplied by the arterial network, a single-input model may be considered, given that the portal venous supply is typically very small.

A dual-compartment model assumes that the contrast agent is distributed between two compartments, the vascular space and the extravascular-extracellular space (EES), that is, interstitial space. In the normal liver, a single-compartment model could be considered, assuming that the interstitial space (space of Disse) communicates freely with the sinusoids through large fenestration. However, this assumption is not true for the diseased liver (Materne et al. 2000). For example, in liver fibrosis, the deposition of collagen causes an alteration in the sinusoidal architecture (loss of fenestration) and increases resistance to the sinusoidal flow, requiring a dual compartment model to describe the regional microcirculatory alterations (Pandharipande et al. 2005).

The model-based approach allows the calculation of quantitative parameters besides arterial and portal liver perfusion and hepatic perfusion index (HPI), such as regional blood flow (BF, blood flow per unit volume/mass of tissue),

regional blood volume (BV, a fraction of tissue that consists of flowing blood), mean transit time (MTT, averaged time for blood to traverse the tissue vasculature), permeability surface area product (PS, reflecting the diffusion of contrast agent across the capillary endothelium and the surface area of the endothelium) (Miles et al. 2012; Kim et al. 2014) (Fig. 1).

The use of such quantitative parameters as imaging biomarkers in longitudinal studies requires an important prerequisite which is the estimation of the measurement repeatability/reproducibility, which reflects the consistency of the acquisition technique, image post-processing and the data analysis (Bretas et al. 2017). The reported coefficient of variations from previous pre-clinical and clinical studies is less than 5% for perfusion measurements suggesting that this technique can provide robust quantitative parameters (Sahani et al. 2007; Kan et al. 2005; Stewart et al. 2008).

The disadvantages of liver CTPI include limited anatomical coverage and high radiation dose.

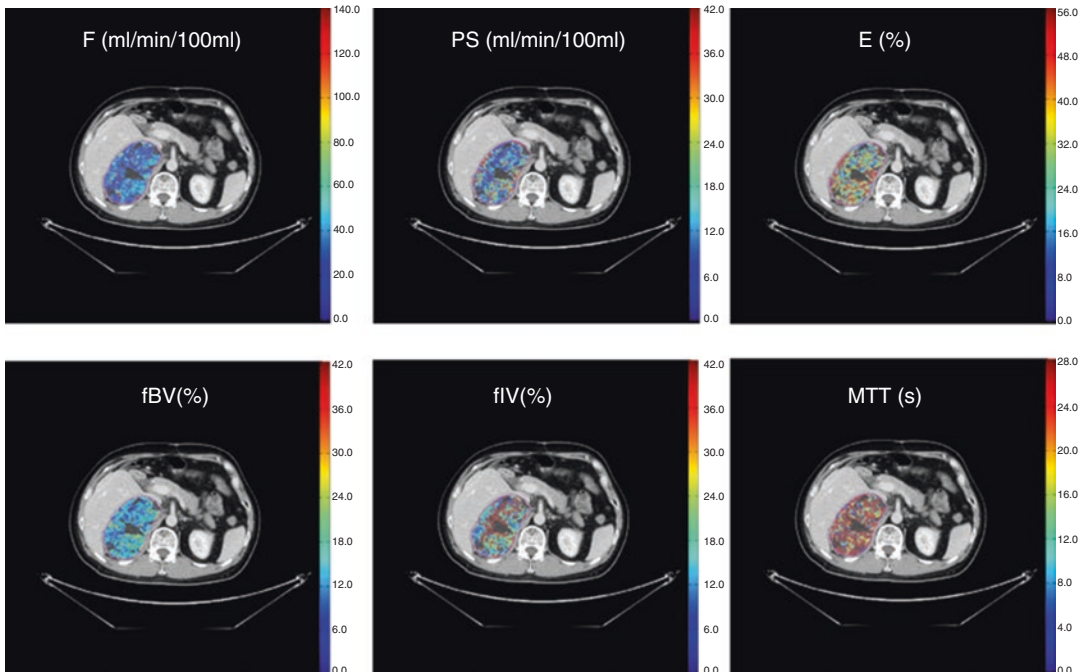


Fig. 1 A middle-age man with hepatocellular carcinoma in the right lobe of the liver underwent perfusion CT imaging. Parametric maps are generated using a dual-input, dual-compartment, distributed-parameter tracer

kinetic model showing F (blood flow), PS (permeability–surface area product), E (extraction fraction), fractional intravascular volume (fBV), fractional interstitial volume (fIV) and mean transit time (MTT)

For this reason, dual-energy CT has been suggested as a potential surrogate for perfusion information. In comparative studies performed in patients with HCC, the quantitative parameter of iodine density determined at dual-energy CT showed good correlation with CTPI derived perfusion parameters (Gordic et al. 2016; Mule et al. 2018). Indeed, the advantage of dual-energy CT is the substantially lower radiation dose when compared to CTPI; however the disadvantage is that acquisition is usually obtained in a single phase, and the lack of information regarding lesion/tissue temporal and peak enhancement can lead to inaccurate results (Gordic et al. 2016).

3.2.1 Clinical Application

Since the first reports in the early 1990s on the usefulness of CTPI in the liver, there has been a wide interest, especially in oncology, for disease detection and characterisation, tumour staging, identification of prognostic biomarkers for patient outcome, assessment of treatment efficacy and in pharmacodynamic evaluation for anti-cancer agent development.

3.2.1.1 Focal Liver Lesions

In patients with chronic liver disease and at high risk for HCC, imaging is used to detect and characterise small hepatic nodules (< 2 cm). Increased arterialisations of early HCC can be detected by contrast-enhanced imaging, which contributes to the differentiating between benign/premalignant and malignant nodules. The overall sensitivity of detecting HCC nodules using multiphase CT has been reported between 54-87%, and this decreases to 45-57% for nodules less than 2 cm. By using CTPI to quantify lesion arterial and portal perfusion, a higher detection rate of 92-98% has been reported (Fischer et al. 2015).

During carcinogenesis, an increase in the hepatic arterial perfusion and HPI, together with a decrease hepatic venous perfusion are signs of malignant transformation of dysplastic nodules into HCC (Matsui et al. 2011; Ippolito et al. 2012). A sensitivity of 100% using a cut off of $\geq 99\%$ HPI and a specificity of 100% using a cut off of $\geq 85\%$ HPI for the diagnosis of HCC have

been reported (Fischer et al. 2015). The BF, BV and MTT also have prognostic value in patients with HCC: tumour with high BF and BV and low MTT, suggesting high vascularity and extensive arteriovenous shunts, are associated with poorer prognosis (Jiang et al. 2012; Petralia et al. 2011).

In livers with occult micro-metastases, increased hepatic arterial perfusion and HPI and decreased PVP have been observed due to the hemodynamic changes secondary to the formation of new, unpaired arterial vessels. These observations reported in both pre-clinical and clinical studies suggest that CTPI may be used to predict the presence of micro-metastases in patients at a high risk in whom conventional imaging modality may have limited diagnostic sensitivity because of the lack of associated morphologic changes (Tsushima et al. 2001; Cuenod et al. 2001). Indeed, early detection of liver metastasis can have important implications for treatment management and patient prognosis.

Several studies have investigated the use of CTPI for characterising focal hepatic lesions based on their perfusion properties. Hepatic metastases from colorectal cancer, for example, which receive their vascular supply principally through the arterial network, show an increased hepatic arterial perfusion and decreased portal venous perfusion at CTPI (Reiner et al. 2012). Hepatic metastases from neuroendocrine tumours demonstrate significantly higher HPI, BF, BV, PS, and significantly shorter MTT compared with the non-tumoural liver parenchyma (Guyennon et al. 2010). Moreover, there is anecdotal evidence that CTPI parameters such as increased HPI or decreased portal vein perfusion may confer a poor prognostic in patients with colorectal liver metastases although this requires further validation (Leggett et al. 1997; Miles et al. 1998).

Another application for CTPI is for the evaluation of treatment efficacy. Vascular targeting anti-cancer agents used in combination with conventional systemic treatment or as monotherapy, in several tumour types. These drugs arrest tumour progression by inhibiting vascular formation thus inducing a cytostatic more than a cyto-

toxic effect and as a consequence, there may be minimal morphologic or size measurement changes. Recent studies showed a significant reduction in the BF and BV and increased MTT in responders to therapy without significant size, in both the pre-clinical and clinical setting, suggesting that these parameters could be considered for monitoring treatment response and also as potential early predictive biomarkers of response (Ren et al. 2012; Ng et al. 2011; Yang et al. 2012; Ng et al. 2018). In both hepatic metastases and HCC nodules treated with radiofrequency ablation (RF), a decrease of HPI of more than 73% in the central necrotic zone and more than 76% in the transitional zone assessed 24 h after RF was associated with a complete response with an AUC of 0.911 (Marquez et al. 2017). Although highly promising, CTPI quantitative parameters cannot yet be used to direct patient management as further validation needs to be acquired from large and multicentric prospective studies (Kim et al. 2014).

3.2.1.2 Diffuse Liver Disease

Liver fibrosis is a diffuse cicatrization process related to chronic liver damage, which can be induced by viral, genetic, metabolic and autoimmune aetiologies. The severity of liver damage is based on the histological analysis of the necroinflammatory activity present on liver biopsy specimens and is graded from A0 (absent) to A3 (severe), as well as fibrosis graded from F0 (absent) to F4 (cirrhosis) (Bedossa and Poynard 1996). Cirrhosis represents the end-stage of liver fibrosis progression and is a predisposing condition for liver failure and increases the risk for HCC (Schuppan and Afdhal 2008).

Important microcirculatory changes occur in liver fibrosis and cirrhosis. There is increased intrahepatic vascular resistance with a secondary decrease in portal venous inflow compensated by an increased arterial inflow (Lautt 1985; Tsushima et al. 1999). Hence, CTPI can be used to increased hepatic arterial perfusion and decreased portal venous perfusion, together with reduced total liver perfusion associated with cirrhosis (Miles et al. 1993; Materne et al. 2000; Van Beers et al. 2001). Moreover, for discrimi-

nating minimal (F1) from the intermediate stage of fibrosis (>F2), the MTT was found to be discriminatory in this setting (Ronot et al. 2010).

3.3 Dynamic Contrast-Enhanced MR Imaging (DCE-MRI)

Perfusion imaging can be undertaken using CT and MRI. For hepatic MR perfusion, several techniques may be deployed. Typically, intravenous contrast is administered for DCE-MRI and T1-weighted sequences are used to track the passage of gadolinium contrast media through tissues. However, there are also non-contrast techniques. Intra-voxel incoherent motion (IVIM) applies diffusion-sensitising magnetic field gradients to the MR imaging sequence, which does not require contrast agent administration. Likewise, the arterial spin labelling technique is based on observing magnetically labelled proximal endogenous water in arterial blood, as this water freely diffuses into the tissue.

Compared with CTPI, DCE-MRI has several advantages including the lack of radiation, higher contrast-to-noise ratios and multiparametric capabilities. DCE-MR imaging can provide information on the microcirculatory characteristics of the tissue by probing low molecular weight gadolinium (gd)-based contrast agents, as they leak from the vascular space into the extravascular extracellular space (EES) and is then eliminated by the kidneys. As the contrast agent transits through the tissue, changes in T1 signal are observed.

Semi-quantitative parameters can be extracted from the signal intensity-time curve and include area under the curve (AUC) which provides the amount of enhancement over a defined period, the peak enhancement ratio, time to peak, steepest slope and the mean transient time (MTT) (Evelhoch 1999). This approach although straightforward has a number of limitations: the calculated parameters do not accurately reflect contrast agent concentration in the tissue, they are highly dependent on the imaging acquisition protocols and the scanner properties and they

provide no insight into the underlying physiology (Padhani 2002; Yankeelov and Gore 2009).

Conversion of signal intensity (SI) changes versus time into contrast agent concentration changes versus time curves allows the use of tracer kinetic modelling and the calculation of microcirculatory quantitative parameters. The general approach to model the changes of Gd-based contrast agent concentration is similar to that developed for the diffusible tracer. Since these contrast agents do not penetrate the cells, the exchange occurs between the vascular compartment and the interstitial space (EES). Hence, changes in the tissue of contrast agent concentration are given by combining the changes in the EES and the changes in the plasma concentration, namely the arterial (vascular) input function (AIF) (Tofts 1997).

There are some technical requirements that should be considered and respected when applying DCE-MR to investigate the liver/lesion perfusion that includes robust acquisition techniques using high temporal resolution, estimation of gd-based contrast agent concentration using multiples flip angles techniques and measuring both the arterial and the venous vascular inputs since, as said previously, the liver is supplied by the hepatic artery and the portal vein (Buckley 2002). To obtain high temporal resolution images (<3 s) of the liver, three-dimensional gradient-echo weighted sequences are most commonly used. However, more recently there is increased interest in motion-resistant sequences (i.e. Radial-VIBE or CAIPIRINHA-VIBE) which may provide high-quality images from free-breathing sequences. Low molecular weight (<1000 Da) chelates of gadolinium that exchange relatively fast with the interstitial space should be administered using a power injector to assure the reproducibility of the injection.

As for CTPI, from a modelling perspective, a dual-input function (dual-AIF) should be considered for the liver as the tracer input into the model will come from both the hepatic artery and the portal vein (Materne et al. 2002). By doing so, the use of a more complex modelling approach such as dual-input, dual-compartment and distributed parameter model can be applied

(46). The following quantitative parameters can be obtained using a dual vascular input and a bi-compartmental model (vascular and interstitial space): K_{trans} (transfer constant) which represents vascular permeability in a permeability-limited (high-flow) situation or blood flow in a flow-limited situation, the K_{ep} (reverse flux rate constant) which estimates the return process of the contrast agent from the EES to the intravascular space, and v_e , which reflects the volume fraction of EES (Thng et al. 2014; Sourbron 2010).

3.3.1 Clinical Applications: Diffuse and Focal Liver Diseases

DCE-MR has been widely used in clinical trials to provide imaging biomarkers for diffuse liver diseases such as liver fibrosis and cirrhosis and to monitor anti-angiogenic drug efficacy on hepatic metastases or hepatocellular carcinoma (Hagiwara et al. 2008; Liu and Matsui 2007). Most of these studies have used IAUC (model-free approach) (Fig. 2.) and/or a single-input, dual-compartment model (Tofts model) in which K_{trans} (transfer constant) and v_e were calculated.

DCE-MR imaging can provide non-invasive semi-quantitative and quantitative perfusion-related parameters that correlate with the stage of liver fibrosis: with increasing fibrosis, there is a decrease in the portal fraction and an increase in the arterial enhancement fraction to increase (Patel et al. 2010; Ou et al. 2013; Bonekamp et al. 2012; Kim et al. 2008). These microcirculatory changes become more marked in cirrhotic livers where they also correlate with the degree of liver dysfunction and portal hypertension (Annet et al. 2003). The diagnostic performance of DCE-MR increases with the severity of fibrosis (Petitclerc et al. 2017).

Similar to CTPI, DCE-MR has been used to assess the treatment efficacy of anti-cancer agents. Vascular targeting anti-cancer drugs such as anti-angiogenic and vascular-disruption agents act on the tumour vascularisation (Fig. 3). In advanced HCC treated with sorafenib combined with tegafur/uracil, a reduction of K_{trans} was associated with improved progression-free

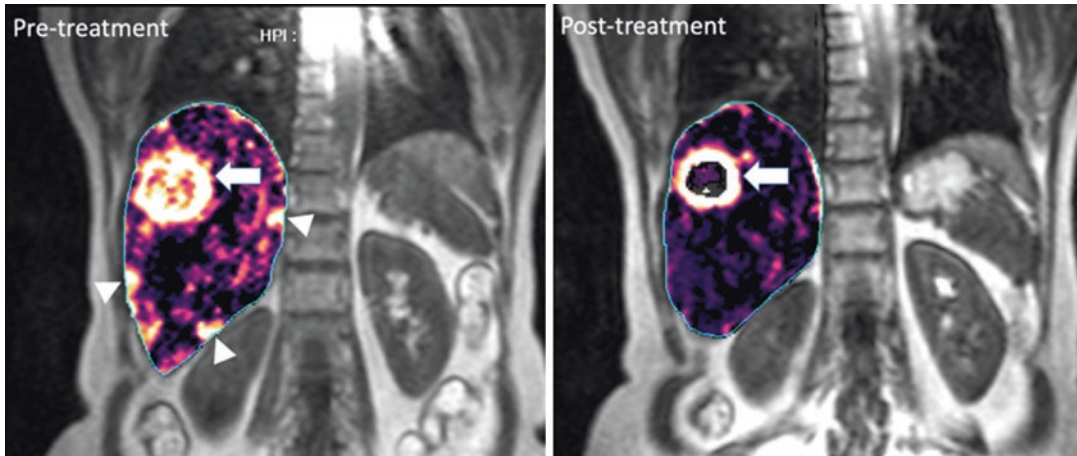


Fig. 2 Hepatic perfusion index. A woman with metastatic neuroendocrine tumour. Semi-quantitative hepatic perfusion index (HPI) maps obtained before and after 12 weeks of octreotide treatment. Pre-treatment HPI map shows a dominant metastasis (arrow) in the right lobe of the liver,

with smaller metastases (arrowheads) in the peripheral of the liver showing high HPI values. Note the HPI reduction in the centre of the dominant metastasis after therapy, as well as in the smaller peripheral metastases

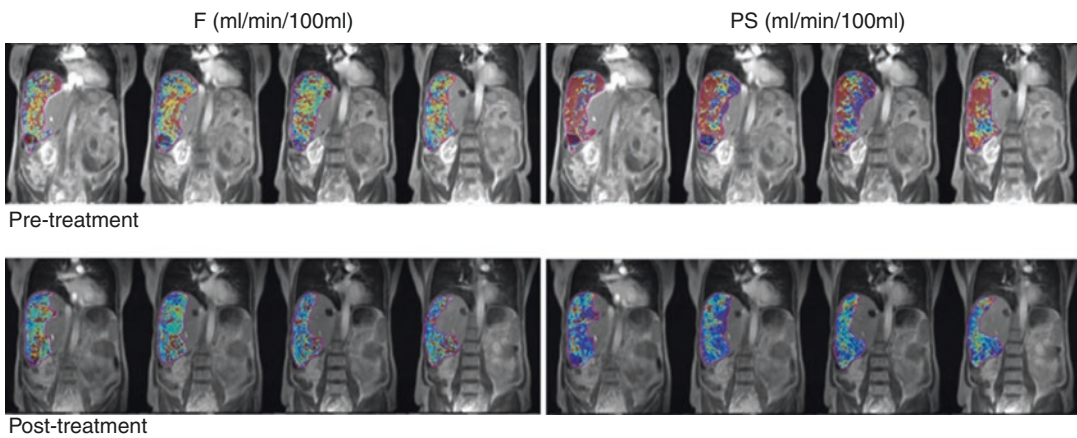


Fig. 3 Quantitative response of tumour to treatment. Parametric blood flow (F) and permeability-surface area product (PS) maps overlaid on T1-weighted images in a patient with hepatocellular carcinoma. Pre-treatment images show high F (58.11) and PS (33.16) values within

the large tumour in the right lobe of the liver. Post-treatment images following targeted therapy shows a slight reduction in tumour size but significant reduction in the F (50.81) and PS (13.2) values, in keeping with treatment response

survival and overall survival (Hsu et al. 2011). Moreover, in HCC treated with sunitinib, perfusion parameters were more accurate to predict early response and progression-free survival than RECIST 1.1 and mRECIST (Sahani et al. 2013). In patients with colorectal liver metastases treated with Regorafenib monotherapy, DCE-MR derived parameters such as KEF (summarised median values of K_{trans} and EF

(enhancing fraction)) demonstrated predictive value for response assessment and was significantly associated with progression-free and overall survival. Patients responding to the treatment demonstrated a significant drop of KEF on day 15 after treatment initiation and significantly better PFS and OS compared to non-responders where no changes in KEF were observed (Khan et al. 2018).

4 Assessing Cellularity and Microstructural Organisation

4.1 Background Considerations

Diffusion-weighted MRI (DWI) is now an established technique for imaging the liver (Taouli and Koh 2010). Using a single-shot echo-planar technique, DWI can be performed rapidly in the liver using a breath-hold, respiratory-triggered or free-breathing imaging technique, providing high contrast between areas of impeded diffusion against the normal liver parenchyma (Koh and Collins 2007). In clinical practice, DWI is widely used as an inherent contrast mechanism to help detect focal liver lesions, especially liver metastases and HCC, without the need for intravenous contrast administration. However, there is interest in developing quantitative DWI to improve disease assessment.

Depending on the number and the range of diffusion weightings (b-values) used for image acquisition, different quantitative parameters can be derived that can inform disease assessment. The most widely used quantitative parameter derived is the apparent diffusion coefficient (ADC), which assumes a monoexponential relationship between the image signal attenuation with increasing b-value. The ADC value is reduced in areas of increased cellularity (e.g. liver tumours) and/or increased microstructural complexity that impede water diffusion (e.g. liver fibrosis or cirrhosis) (Koh and Collins 2007).

However, by using multiple b-values (typically more than 5) including three or more at lower b-values (≤ 150 s/mm²), a biexponential relationship between the image signal and b-values is observed in tissues. This occurs because of intravoxel incoherent motion (IVIM), which results in higher tissue signal attenuation at lower b-values due to the nulling of the protons associated with capillary perfusion (Koh et al. 2011). Hence, using IVIM technique enables the calculation of a diffusion coefficient (D) that reflects tissue diffusivity, a pseudo-diffusion coefficient (D^*) that reflects the rate of tissue perfusion, as well as the perfusion fraction, which

reflects the amount of tissue perfusion. More recently, there has also been an interest in diffusion kurtosis imaging (DKI), which requires diffusion-weighted imaging performed using multiple b-values but including at least one very high b-value (>1500 s/mm²) to study the non-Gaussian behaviour of water diffusion, which is likely to better reflect microstructural organisation, membrane integrity and intracellular water (Rosenkrantz et al. 2015). Using a DKI model, a diffusion coefficient (D) and the diffusion kurtosis (k) can be calculated (Fig. 4).

The ADC is a robust measurement that is highly repeatable in the liver. In well-conducted studies, the coefficient of repeatability of ADC in the normal liver is of the order of less than 10%, which increases to less than 15 to 20% in liver tumours, which may reflect the heterogeneous nature of liver tumours (Andreou et al. 2013; Winfield et al. 2017). The ADC value is also reproducible across vendor platforms. In one study, the coefficient of reproducibility of ADC across vendor systems was found to be approximately 14% for normal abdominal organs (Donati et al. 2014). By contrast, perfusion sensitive IVIM parameters generally show poor measurement repeatability and reproducibility, especially for focal liver lesions, which has limited their wider deployment in the clinical setting (Andreou et al. 2013). The perfusion fraction, f , has better measurement repeatability and reproducibility compared with the pseudo-diffusion coefficient D^* . There may be some merits of using the perfusion fraction f to evaluate disease in specific disease settings, which will be discussed later. There has been limited experience in the measurement repeatability of k in the liver and more work is needed to determine its potential value for disease assessment.

4.2 Clinical Applications

4.2.1 Focal Liver Lesions

Diffusion-weighted MRI provides excellent contrast for the detection of focal liver lesions. The combination of DWI with gadoxetate-enhanced MRI has been shown to result in the

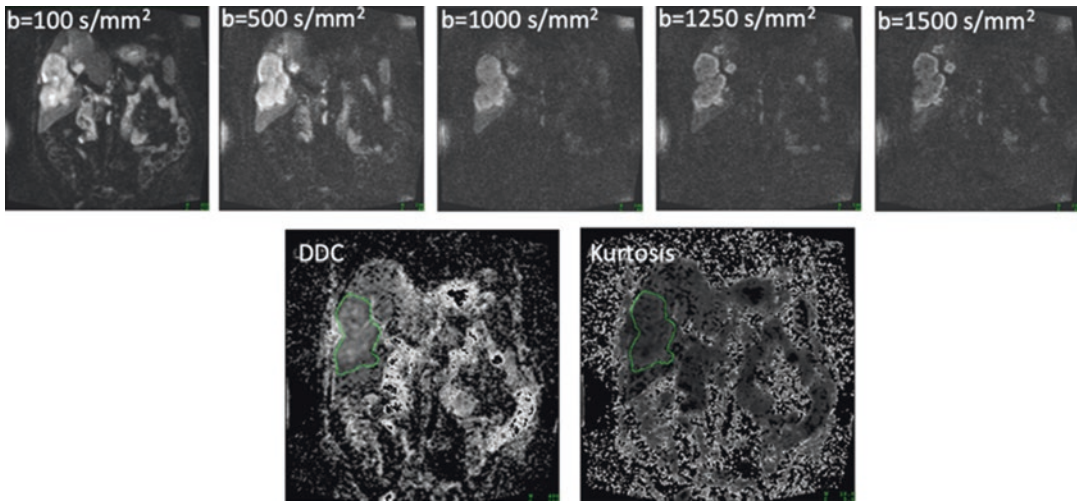


Fig. 4 Diffusion Kurtosis Imaging. Diffusion-weighted imaging using multiple b-values including high b-value (≥ 1500 s/mm²) allows the application of a diffusion kurtosis model to measure the direct diffusion coefficient (DDC) and the kurtosis (K) value. Note that in this patient

with liver metastasis in the right lobe of the liver, the tumour returns slightly higher DDC and K values compared with the adjacent liver parenchyma. (Courtesy: Mihaela Rata, Royal Marsden Hospital, UK)

highest diagnostic accuracy for the detection of liver metastases (Vilgrain et al. 2016). DWI is also highly sensitive for visualising neuroendocrine liver metastases (Ronot et al. 2018) (Fig. 5). DWI facilitates the detection of HCC, including smaller (Park et al. 2012; Le Moigne et al. 2012) (<2 cm in size) and hypovascular (Di Pietropaolo et al. 2015) lesions, although lesion detection depends on the tumour grade and the severity of background cirrhosis (Jiang et al. 2017a).

The ADC value has been employed for the characterisation of focal liver lesions. Benign lesions have been shown to have higher ADC values than malignant lesions. Liver haemangiomas have been shown to have the highest ADC values amongst solid hepatic lesions. A threshold of approximately 1.7×10^{-3} mm²/s has been found to have relatively high sensitivity and specificity (Taouli and Koh 2010). However, this threshold has to be applied with caution and in conjunction with all available imaging findings, as there is substantial overlap in the ADC values of solid liver lesions. For example, the ADC values of focal nodular hyperplasia and adenomas can overlap with the ADC values of HCC and cholangiocarcinomas.

The ADC value is potentially useful for assessing therapeutic effects (Fig. 6). Studies have shown that the ADC value increases in responders to chemotherapy, radiotherapy, embolisation therapy or minimally invasive treatments (Padhani and Koh 2011; Kokabi et al. 2015). Such an ADC increase has been shown to occur as early as 7 to 14 days following the commencement of treatment, providing an early biomarker to therapeutic effects. For this reason, the ADC value is being applied as a potential readout for assessing the effectiveness of novel therapeutics.

Using IVIM MRI, one study evaluated 74 patients with 75 lesions, of which 51 were malignant and 24 benign. The diffusion coefficient (D) and perfusion fraction (f) were found to be significantly lower in malignant than benign lesions. Nonetheless, D was found to be still more accurate than f for this purpose (Luo et al. 2017). IVIM MRI was also shown to help discriminate between different grades of HCC (Granata et al. 2016); as well as between HCC and intrahepatic cholangiocarcinomas (Shao et al. 2019). A recent meta-analysis (Wu et al. 2018) evaluated 484 patients with 582 liver lesions, including 381 malignant and 201 benign lesions. The authors found that ADC and

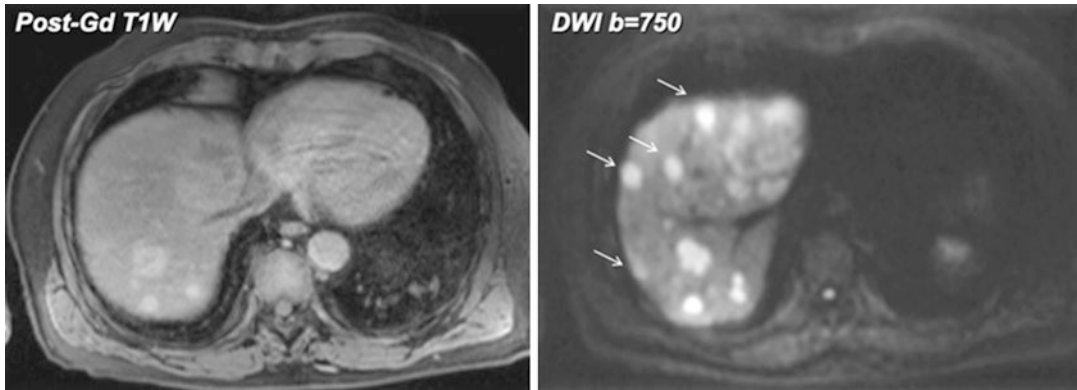


Fig. 5 Detection of neuroendocrine liver metastases. Diffusion-weighted imaging improves the detection of neuroendocrine liver metastases. Portovenous phase MRI following intravenous gadolinium contrast administration

shows several enhancing metastases in the right lobe of the liver. However, diffusion-weighted imaging demonstrates many more lesions (arrows) within the liver, not visualised on contrast-enhanced MRI

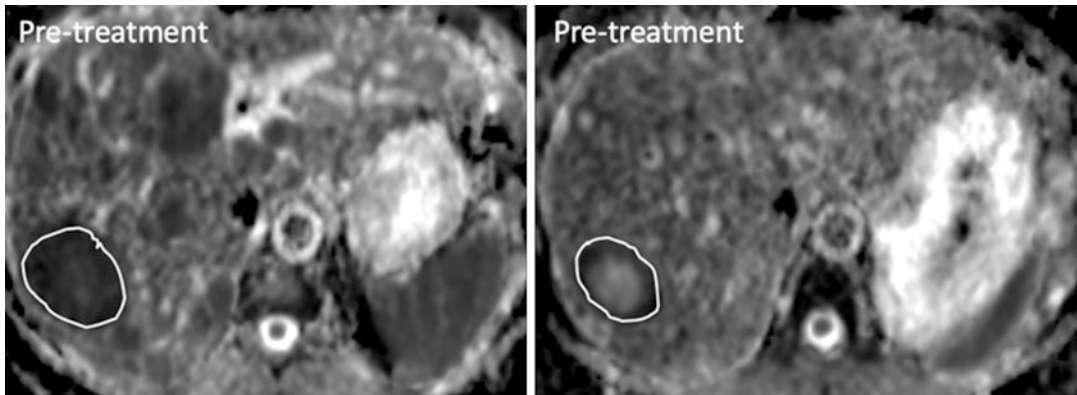


Fig. 6 Change in ADC in responders to treatment. ADC maps in a man with neuroendocrine liver metastasis before and after Y90-Dotatate treatment. The liver metastasis shows a mean ADC value of 0.89×10^{-3} s/mm²

before treatment, increasing to 1.54×10^{-3} s/mm² after treatment, representing a 73% increase in the ADC value, in keeping with treatment response. Note that there is only a slight reduction in the tumour size after treatment

D values were significantly higher in benign lesions, while there was no significant difference in the D^* and f values between the benign and malignant lesions. The heterogeneity of the IVIM results may relate to the techniques applied which impacts the repeatability and reproducibility of the perfusion sensitive parameters. In this regard, meticulous technique to ensure good image signal-to-noise and careful choice of model fitting should be advocated in future studies. IVIM has also been used to evaluate the treatment response of liver metastases, which revealed a reduction in the perfusion fraction in responders to treatment (Granata et al. 2015; Kim et al. 2016).

4.2.2 Diffuse Liver Disease

Diffuse and focal steatosis can lead to a lowering of the ADC value of the liver parenchyma (Murphy et al. 2015; Dijkstra et al. 2014; Guiu et al. 2012). In patients with chronic liver disease, liver fibrosis and cirrhosis also lower the ADC value of hepatic parenchyma, which aids the detection of fibrosis/cirrhosis (Jiang et al. 2017b). It has been found that patients with higher grades of liver fibrosis (F3, F4) have lower ADC values than those with lower grades of liver fibrosis (F1, F2). However, the differences in the ADC values between these categories may be relatively small in relation to the

measurement repeatability. This means that on a practicable basis, it is unclear to what extent the ADC value may have sufficient dynamic range to confidently discern between the different degrees of hepatic fibrosis.

IVIM DWI has been also applied to evaluate hepatic cirrhosis. The diffusion coefficient (D) and perfusion fraction (f) have been shown to decrease with fibrosis and cirrhosis (Franca et al. 2017; Ichikawa et al. 2015; Yoon et al. 2014). Using DKI, studies have also shown that the kurtosis value (k) is directly correlated with the degree of liver fibrosis (Yoon et al. 2019; Yang et al. 2018). However, the performance of IVIM DWI and DKI are poorer than MR elastography for the diagnosis and staging of liver fibrosis (Ichikawa et al. 2015).

More recently, it has been suggested that diffusion-weighted MRI may be used as a method to measure the elasticity of liver tissue (virtual elastogram), without the need for the use of an external drive. The calculation of the shifted ADC (sADC) has been shown to correlate with the shear modulus derived from MR elastography ($r^2 = 0.9$). However, this approach requires further validation (Le Bihan et al. 2017).

5 Assessing Tissue Elasticity and Stiffness

5.1 Background Consideration

Magnetic resonance elastography (MRE) is a functional imaging technique that is used to quantify the elasticity of soft tissues by visualising the propagation of shear waves, usually generated using an external driver, using a modified phase-MRI sequence. The use of MRE is akin to “virtual palpation”, which aims to differentiate tissues based on their tissue stiffness. MRE is an accurate method for the detection and staging of liver fibrosis, although its use is often limited to specialist centres as dedicated hardware and software are needed to implement the technique on MRI systems.

MRE can be performed at both 1.5 T and 3.0 T, although it appears to be more robust at 1.5 T across different vendor systems. MRE examination requires an actuator, which uses mechanical excitation positioned against the body to generate compression waves, which are translated into transverse shear waves in the body. The actuator used to generate the compression waves can be pneumatic, electromechanical or piezoelectric. The shear waves that are propagated in the body are imaged using a phase-contrast MRI technique that includes oscillating motion sensitising gradients, of which gradient-echo, spin-echo echo-planar sequences are frequently used. A meta-analysis revealed that both gradient-echo and spin-echo echo-planar techniques performed equally in the evaluation of liver fibrosis (Kim et al. 2018). The phase shift in the MRI signal in tissues is used to generate the wave image, and by using an inversion algorithm, the wave images are transformed into elastograms of tissue stiffness.

Studies have liver MRE has good measurement repeatability (intraclass coefficients) and inter-rater agreement (Shire et al. 2011; Lee et al. 2014). In one meta-analysis, a 22% or greater change in the mean liver stiffness evaluated over the same region using the same technique indicates that a real change has occurred with 95% confidence (Serai et al. 2017). MRE measurement of liver stiffness was not found to be influenced by age, gender, body-mass index (Singh et al. 2015) or the administration of gadolinium contrast medium (95). However, liver stiffness is affected by prandial state (Hines et al. 2011), and hence, liver MRE should be measured following a period of fasting. A good intra-class correlation coefficient (ICC) of 0.9 (95%CI: 0.78-0.96) and a within-subject coefficient of variation of 2.2%-11.4% have been reported for MRE liver stiffness measurements (Singh et al. 2015; Wang et al. 2018). The mean liver stiffness also showed good measurement reproducibility in a study across two vendor systems; showing a mean difference of 0.09 KPa, and a coefficient of repeatability of 0.25 KPa for the mean liver stiffness (Serai et al. 2015).

5.2 Clinical Applications

5.2.1 Focal Liver Lesions

MRE has been applied to characterise focal liver lesions. A preliminary study involving 44 liver tumours (which included metastases-14, hepatocellular carcinoma- 12, hemangioma-9, cholangiocarcinoma-5, focal nodular hyperplasia-3, and hepatic adenoma-1) found that MRE could distinguish tumours as malignant or benign with 100% accuracy, using a stiffness threshold of 5 kPa at 60 Hz (Venkatesh et al. 2008). More recently, in a study of 79 patients with 80 malignant and 44 benign focal liver lesions, MRE was found to be superior to diffusion-weighted imaging (DWI) for differentiating between malignant and benign pathologies (Hennedige et al. 2016). Malignant lesions showed a higher mean stiffness (7.9 kPa vs. 3.1 kPa) but lower mean ADC value (1.29 vs. 2.00×10^{-3} mm²/s) compared with benign lesions (100). However, ROC analysis showed higher diagnostic accuracy for MRE than DWI (0.986 vs. 0.82) (Hennedige et al. 2016).

5.2.2 Diffuse Liver Disease

The patients with suspected liver fibrosis, liver biopsy is confirmatory but is highly invasive and is associated with sampling errors and potential risk of complications. For this reason, non-invasive diagnosis of liver fibrosis is attractive, which can also be used to monitor the evolution of the disease. Biopsy can also be targeted towards where fibrosis is most severe on imaging (Perumpail et al. 2012).

Multiple studies have confirmed the value of MRE for the non-invasive evaluation of liver fibrosis (Fig. 7). In one recent meta-analysis of 26 studies with a total of 3200 patients, the authors found no significant difference in the pooled sensitivity and specificity of MRE using either a gradient-echo or a spin-echo EPI technique. The area under the receiver operator characteristic curve for the stage diagnosis of any ($F \geq 1$), significant ($F \geq 2$), advanced ($F \geq 3$), and cirrhosis ($F = 4$) on gradient-echo MRE and spin-echo echo-planar MRE were 0.93 versus 0.94, 0.95 versus 0.94, 0.94 versus 0.95, and 0.92

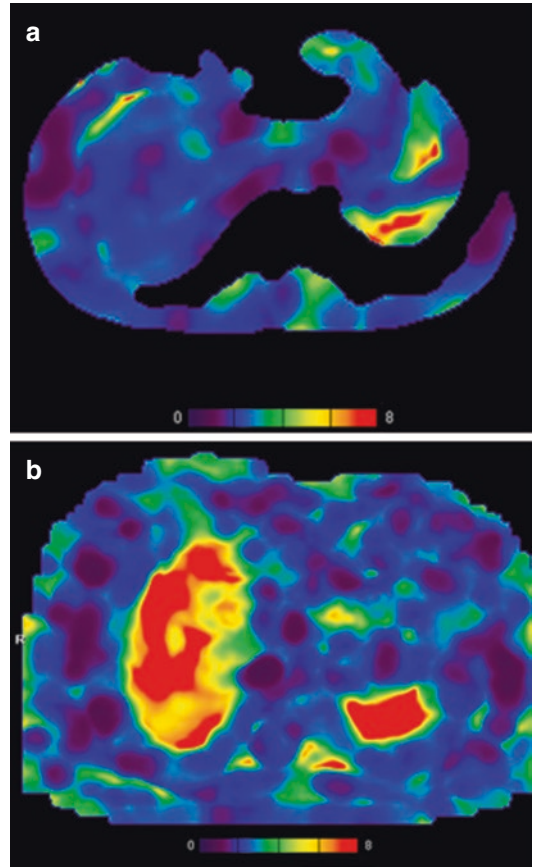


Fig. 7 Shear-wave elastography of (a) a normal liver and (b) man with Metavir grade F4 liver cirrhosis showing increased liver stiffness (in kPa) in the small cirrhotic liver (Courtesy: Dr. Albert Low, Singapore General Hospital)

versus 0.93, respectively (90). MRE was also more accurate for diagnosing liver fibrosis compared with transient elastography or point shear wave elastography (Perumpail et al. 2012). Using a threshold of 2.93 kPa at 60 Hz, Yin et al. (2007) found that MRE had 98% sensitivity, 99% specificity and 97% negative predictive value for liver fibrosis. Interestingly, the performance of MRE for staging liver fibrosis appears to be independent of the aetiology of the disease.

MRE has also been used to study the effects of treatment that modulates liver fibrosis. In one study (Jayakumar et al. 2019), 54 patients with MRE and liver biopsies at baseline and week 24 were treated with selonsertib, an inhibitor of apoptosis signal-regulating kinase 1 (ASK1),

which has anti-inflammatory and anti-fibrotic properties. In that study, 18 (33%) had fibrosis improvement (≥ 1 -stage reduction) after undergoing 24 weeks of treatment with the study drug. The area under the receiver operating characteristic curve of MRE-stiffness to identify improvement in the fibrosis score was 0.62 (95% CI 0.46-0.78) and the optimal threshold was a $\geq 0\%$ relative reduction. Applying this threshold, MRE had 67% sensitivity, 64% specificity, 48% positive predictive value, 79% negative predictive value.

In addition, MRE has been applied to observe changes in liver stiffness in patients with non-alcoholic fatty liver disease (NAFLD). Several studies have demonstrated an increase in liver stiffness in patients with non-alcoholic steatohepatitis (NASH), in the absence of fibrosis. In one study, using a threshold of 2.74 kPa (Chen et al. 2011), MRE showed high diagnostic accuracy for identifying patients with NASH from patients with simple steatosis with an area under the ROC curve of 0.93. However, the practical application of MRE in this clinical context requires further validation.

6 Evaluation of Liver Function

6.1 Background

Chronic liver parenchymal disease leads to hepatocellular dysfunction, which eventually manifests as deranged serum liver function tests. However, the loss of normal liver function can be heterogeneous, segmental or sub-segmental, which may not be appreciated from serum findings. The ability to visualise the extent and distribution of liver dysfunction may be useful for treatment planning.

Following the administration of a hepatocyte selective contrast medium (e.g. gadoxetic acid), approximately 50% of gadoxetic acid is taken up by hepatocytes during the transitional and hepatobiliary phase of contrast enhancement by transmembrane transporters such as the organic anion transporting polypeptides OATP1 B1/B3 present on the sinusoidal membrane of the hepa-

toocytes. The excretion of contrast into the biliary system occurs through the MRP2 transporters. Hence, the T1-enhancement of liver parenchyma following gadoxetic acid contrast administration can reflect hepatocyte function.

To measure hepatocyte function, quantification of the T1-relaxivity of hepatic parenchyma is performed before and at 10 to 20 min following gadoxetic acid contrast administration. There are several imaging sequences that have been applied, including a modified Look-Locker inversion recovery (MOLLI) technique or a variable flip angle (VFA) gradient-echo technique. These sequences may be executed with or without correction for the B1-field inhomogeneity. Studies have shown that the magnitude of change in the T1-relaxation time following contrast administration is highly reflective of the underlying liver excretory function, which can be used to produce parametric maps of hepatocellular function. Although the native T1 value of the liver is reduced in patients with liver cirrhosis (Cassinotto et al. 2015), this is not sufficiently discriminatory to identify patients with impaired liver function.

Measurement of the T1-relaxation time in the liver is highly repeatable (107). In one study, the within-subject coefficient of variance for T1 measurement of the liver was found to be 0.3% before gadoxetate contrast administration, and 1.1% after gadoxetate administration. However, significant variation is encountered in the T1-relaxation time of the liver when different T1-measurement techniques are applied. For example, there is significant variance in the T1 measurement between using MOLLI sequence versus the VFA technique (Yoon et al. 2016; Yoon et al. 2017).

6.2 Clinical Application

6.2.1 Evaluating Liver Function

Currently there is no consensus on which MR-derived parameters should be used to assess liver function by gadoxetate-enhanced MRI (Bae et al. 2012). Relative liver enhancement (RLE), contrast enhancement index and hepatic uptake index (HUI) are parameters based on single

intensity (SI) measurements, which are relatively easy to derive (Watanabe et al. 2011). Measurement of the T1 relaxation time is more accurate than SI measurements, given the more direct relationship between T1 relaxation times and contrast agent concentration, although this relationship is more complex using gadoxetate, as the contrast is distributed in different compartments (i.e. intracellular and in the bile) (Besa et al. 2015). There is also considerable variation in the T1-relaxation time measurements depending on the imaging sequence/technique applied, the availability of these sequences varies across vendor systems. In addition, there is reportedly segmental variation of the liver T1 value across the liver, both before and after contrast administration (Haimerl et al. 2017). Furthermore, the T1-relaxation time varies with the magnetic field strength, being longer at higher field strength than at lower field strength. For these reasons, there is not yet a universally accepted method to measure or define liver tissue T1 relaxivity.

Nonetheless, it has been found that the change in the T1 relaxation time measured by the same imaging technique before and after gadoxetate contrast administration is highly correlated with liver function. Although the native T1 relaxation time of cirrhotic liver is longer compared with normal liver, this is not predictive of liver function. However, patients that show a small reduction in the T1 relaxation time (expressed as a percentage of the pre-contrast T1 relaxation time) after contrast administration are associated with impairment of liver function (Yoon et al. 2016; Besa et al. 2015; Katsube et al. 2011; Haimerl et al. 2013) (Fig. 8). Other quantitative parameters that have been used to identify patients with impaired liver function include the extracellular enhancement (by comparing with the enhancement of the spleen), functional liver-to-weight ratio and the hepatic uptake ratio (Yoon et al. 2019). One recent study at 3 T showed the hepatic uptake ratio was highly correlated with the ICG-r15 test, in patients with Child-Pugh class A or B liver cirrhosis (Yoon et al. 2019).

One potentially more sophisticated approach is dynamic hepatocyte-specific contrast-enhanced MRI which provides both semi-quantitative and

quantitative parameters. Semi-quantitative parameters such as the maximum enhancement (Emax), time to peak (Tmax) and elimination half-life do not have any clear insight into the underlying physiology. The calculation of quantitative parameters implies the use of pharmacokinetic analysis of the parenchyma- and vascular-input concentration-time curves and include regional BF, regional BV, arterial and portal venous perfusion and hepatocyte extraction fraction (Sourbron et al. 2012). However, this approach requires sophisticated data acquisition and analysis, which can only be undertaken in specialist institutions.

Besides the microcirculatory changes, a decrease in the expression of the hepatocyte organic anion transporters has been observed in liver fibrosis, which can be inferred by using gadoxetate MRI. The reduction in OATP transporters will cause a decrease in the T1-shortening effect of the gadolinium contrast. Quantitative T1 mapping-based hepatocyte fraction demonstrated a strong correlation with fibrosis stages and also showed a good diagnostic performance in identifying patients with advanced liver fibrosis and cirrhosis (Pan et al. 2018).

7 Future Developments

There have been significant advances in MR hardware and software over the years, which have impacted our ability to derive functional imaging data from the liver. As compressed-sensing techniques become mainstream on all vendor MR systems, the ability to acquire high temporal and high spatial-resolution dynamic contrast-enhanced MR images significantly improve the way we perform perfusion MRI and possibly on how we assess liver function using MRI.

One of the major disruptors in imaging is artificial intelligence and deep learning, and there is no doubt that rapid developments in the field improve the speed of image reconstruction for functional imaging, disease segmentation and complex data analysis. One of the current limitations of applying functional imaging

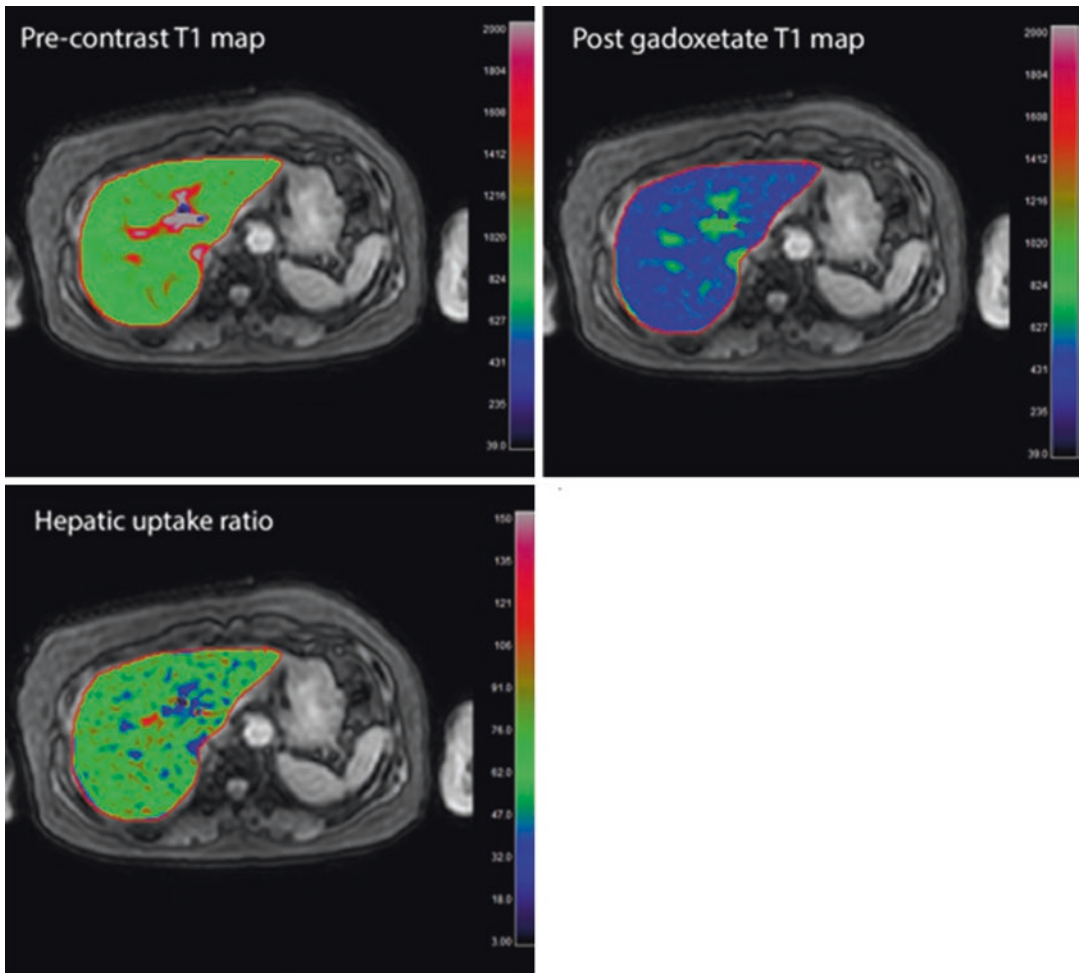


Fig. 8 A 66-year-old woman with hepatitis B and liver cirrhosis (Child-Pughs Class A). Quantitative T1-mapping was performed using a Look-Locker sequence at 3 T before and at 10 mins after gadoxetate-enhanced MRI. The mean pre-contrast T1-value is 978 ms, while the mean post-contrast T1-values is 496 ms. The reduction in

T1-value after contrast indicates a good liver function test. These findings are corroborated with the hepatic uptake ratio map (normalised to splenic uptake), which shows a mean uptake ratio of 70 (Courtesy: Dr. Yoon Jeong Hee, Seoul National University Hospital)

techniques is that many of the image processing steps and data analysis are performed off-line by dedicated physicists and data scientists, which are not accessible to the majority of radiological departments. Using artificial intelligence and machine learning, it may be possible to generate new tools that can undertake in-line processing of complex functional imaging datasets automatically or semi-automatically, so that the quantitative results can be made available at the point of image reading for clinical decision making.

As radiomics analyses continue to generate promising biophysical properties from images that are linked to patients' treatment outcomes or prognosis, there is increasing interest in performing radiomics on MRI datasets. One of the limitations of using MR images for radiomics is that there may be substantial variations in the measured signal according to the patient position within the MRI scanner, which can lead to variations in the results. Currently, different approaches to signal normalisation are being applied to overcome some of these limitations, but there are

advantages in performing radiomics analyses on quantitative maps derived from functional MR imaging measurements, as a way of overcoming the issue of MR signal variations across native acquired morphological images.

The speed of image acquisition can also be speeded up using artificial intelligence and machine learning. Hence, future liver MRI examination time is likely to decrease; which may allow more time to be spent acquiring functional imaging data. The routine use of a multiparametric functional imaging paradigm for liver imaging for patients within our daily clinical workflow may produce new insights into common diseases, and provide new knowledge for disease management.

References

- Andreou A, Koh DM, Collins DJ, Blackledge M, Wallace T, Leach MO et al (2013) Measurement reproducibility of perfusion fraction and pseudodiffusion coefficient derived by intravoxel incoherent motion diffusion-weighted MR imaging in normal liver and metastases. *Eur Radiol* 23(2):428–434
- Annet L, Materne R, Danse E, Jamart J, Horsmans Y, Van Beers BE (2003) Hepatic flow parameters measured with MR imaging and Doppler US: correlations with degree of cirrhosis and portal hypertension. *Radiology* 229(2):409–414
- Axel L (1980) Cerebral blood flow determination by rapid-sequence computed tomography: theoretical analysis. *Radiology* 137(3):679–686
- Bae KE, Kim SY, Lee SS, Kim KW, Won HJ, Shin YM et al (2012) Assessment of hepatic function with Gd-EOB-DTPA-enhanced hepatic MRI. *Dig Dis* 30(6):617–622
- Bedossa P, Poinard T (1996) An algorithm for the grading of activity in chronic hepatitis C. the METAVIR cooperative study group. *Hepatology* 24(2):289–293
- Besa C, Bane O, Jajamovich G, Marchione J, Taouli B (2015) 3D T1 relaxometry pre and post gadoteric acid injection for the assessment of liver cirrhosis and liver function. *Magn Reson Imaging* 33(9):1075–1082
- Bonekamp D, Bonekamp S, Geiger B, Kamel IR (2012) An elevated arterial enhancement fraction is associated with clinical and imaging indices of liver fibrosis and cirrhosis. *J Comput Assist Tomogr* 36(6):681–689
- Bretas EAS, Torres US, Torres LR, Bekhor D, Saito Filho CF, Racy DJ et al (2017) Is liver perfusion CT reproducible? A study on intra- and interobserver agreement of normal hepatic haemodynamic parameters obtained with two different software packages. *Br J Radiol* 90(1078):20170214
- Buckley DL (2002) Uncertainty in the analysis of tracer kinetics using dynamic contrast-enhanced T1-weighted MRI. *Magn Reson Med* 47(3):601–606
- Cassinotto C, Feldis M, Vergniol J, Mouries A, Cochet H, Lapuyade B et al (2015) MR relaxometry in chronic liver diseases: comparison of T1 mapping, T2 mapping, and diffusion-weighted imaging for assessing cirrhosis diagnosis and severity. *Eur J Radiol* 84(8):1459–1465
- Chen J, Talwalkar JA, Yin M, Glaser KJ, Sanderson SO, Ehman RL (2011) Early detection of nonalcoholic steatohepatitis in patients with nonalcoholic fatty liver disease by using MR elastography. *Radiology* 259(3):749–756
- Chiandussi L, Greco F, Sardi G, Vaccarino A, Ferraris CM, Curti B (1968) Estimation of hepatic arterial and portal venous blood flow by direct catheterization of the vena porta through the umbilical cord in man. Preliminary results. *Acta Hepatosplenol* 15(3):166–171
- Cuenod C, Leconte I, Siauve N, Resten A, Dromain C, Poulet B et al (2001) Early changes in liver perfusion caused by occult metastases in rats: detection with quantitative CT. *Radiology* 218(2):556–561
- Di Pietropaolo M, Briani C, Federici GF, Marignani M, Begini P, Delle Fave G et al (2015) Comparison of diffusion-weighted imaging and gadoteric acid-enhanced MR images in the evaluation of hepatocellular carcinoma and hypovascular hepatocellular nodules. *Clin Imaging* 39(3):468–475
- Dijkstra H, Handayani A, Kappert P, Oudkerk M, Sijens PE (2014) Clinical implications of non-steatotic hepatic fat fractions on quantitative diffusion-weighted imaging of the liver. *PLoS One* 9(2):e87926
- Donati OF, Chong D, Nanz D, Boss A, Froehlich JM, Andres E et al (2014) Diffusion-weighted MR imaging of upper abdominal organs: field strength and intervendor variability of apparent diffusion coefficients. *Radiology* 270(2):454–463
- Dvorak HF, Brown LF, Detmar M, Dvorak AM (1995) Vascular permeability factor/vascular endothelial growth factor, microvascular hyperpermeability, and angiogenesis. *Am J Pathol* 146(5):1029–1039
- Evelhoch JL (1999) Key factors in the acquisition of contrast kinetic data for oncology. *J Magn Reson Imaging* 10(3):254–259
- Fischer MA, Kartalis N, Grigoriadis A, Loizou L, Stal P, Leidner B et al (2015) Perfusion computed tomography for detection of hepatocellular carcinoma in patients with liver cirrhosis. *Eur Radiol* 25(11):3123–3132
- Franca M, Marti-Bonmati L, Alberich-Bayarri A, Oliveira P, Guimaraes S, Oliveira J et al (2017) Evaluation of fibrosis and inflammation in diffuse liver diseases using intravoxel incoherent motion diffusion-weighted MR imaging. *Abdom Radiol (NY)*. 42(2):468–477
- Gordic S, Puippe GD, Krauss B, Klotz E, Desbiolles L, Lesurtel M et al (2016) Correlation between dual-energy and perfusion CT in patients with hepatocellular carcinoma. *Radiology* 280(1):78–87
- Granata V, Fusco R, Catalano O, Filice S, Amato DM, Nasti G et al (2015) Early assessment of colorectal

- Cancer patients with liver metastases treated with Antiangiogenic drugs: the role of Intravoxel incoherent motion in diffusion-weighted imaging. *PLoS One* 10(11):e0142876
- Granata V, Fusco R, Catalano O, Guarino B, Granata F, Tatangelo F et al (2016) Intravoxel incoherent motion (IVIM) in diffusion-weighted imaging (DWI) for hepatocellular carcinoma: correlation with histologic grade. *Oncotarget* 7(48):79357–79364
- Guiu B, Petit JM, Capitan V, Aho S, Masson D, Lefevre PH et al (2012) Intravoxel incoherent motion diffusion-weighted imaging in nonalcoholic fatty liver disease: a 3.0-T MR study. *Radiology* 265(1):96–103
- Guyennon A, Mihaila M, Palma J, Lombard-Bohas C, Chayvialle JA, Pilleul F (2010) Perfusion characterization of liver metastases from endocrine tumors: computed tomography perfusion. *World J Radiol* 2(11):449–454
- Hagiwara M, Rusinek H, Lee VS, Losada M, Bannan MA, Krinsky GA et al (2008) Advanced liver fibrosis: diagnosis with 3D whole-liver perfusion MR imaging—initial experience. *Radiology* 246(3):926–934
- Haimerl M, Verloh N, Zeman F, Fellner C, Muller-Wille R, Schreyer AG et al (2013) Assessment of clinical signs of liver cirrhosis using T1 mapping on Gd-EOB-DTPA-enhanced 3T MRI. *PLoS One* 8(12):e85658
- Haimerl M, Verloh N, Zeman F, Fellner C, Nickel D, Lang SA et al (2017) Gd-EOB-DTPA-enhanced MRI for evaluation of liver function: comparison between signal-intensity-based indices and T1 relaxometry. *Sci Rep* 7:43347
- Henderson E, Milosevic MF, Haider MA, Yeung IW (2003) Functional CT imaging of prostate cancer. *Phys Med Biol* 48(18):3085–3100
- Hennedige TP, Hallinan JT, Leung FP, Teo LL, Iyer S, Wang G et al (2016) Comparison of magnetic resonance elastography and diffusion-weighted imaging for differentiating benign and malignant liver lesions. *Eur Radiol* 26(2):398–406
- Hines CD, Lindstrom MJ, Varma AK, Reeder SB (2011) Effects of postprandial state and mesenteric blood flow on the repeatability of MR elastography in asymptomatic subjects. *J Magn Reson Imaging* 33(1):239–244
- Hsu CY, Shen YC, Yu CW, Hsu C, Hu FC, Hsu CH et al (2011) Dynamic contrast-enhanced magnetic resonance imaging biomarkers predict survival and response in hepatocellular carcinoma patients treated with sorafenib and metronomic tegafur/uracil. *J Hepatol* 55(4):858–865
- Ichikawa S, Motosugi U, Morisaka H, Sano K, Ichikawa T, Enomoto N et al (2015) MRI-based staging of hepatic fibrosis: comparison of intravoxel incoherent motion diffusion-weighted imaging with magnetic resonance elastography. *J Magn Reson Imaging* 42(1):204–210
- Ippolito D, Capraro C, Casiraghi A, Cestari C, Sironi S (2012) Quantitative assessment of tumour associated neovascularisation in patients with liver cirrhosis and hepatocellular carcinoma: role of dynamic-CT perfusion imaging. *Eur Radiol* 22(4):803–811
- Jayakumar S, Middleton MS, Lawitz EJ, Mantry PS, Caldwell SH, Arnold H et al (2019) Longitudinal correlations between MRE, MRI-PDFF, and liver histology in patients with non-alcoholic steatohepatitis: analysis of data from a phase II trial of selonsertib. *J Hepatol* 70(1):133–141
- Jiang T, Kambadakone A, Kulkarni NM, Zhu AX, Sahani DV (2012) Monitoring response to antiangiogenic treatment and predicting outcomes in advanced hepatocellular carcinoma using image biomarkers, CT perfusion, tumor density, and tumor size (RECIST). *Investig Radiol* 47(1):11–17
- Jiang H, Chen J, Gao R, Huang Z, Wu M, Song B (2017a) Liver fibrosis staging with diffusion-weighted imaging: a systematic review and meta-analysis. *Abdom Radiol (NY)*. 42(2):490–501
- Jiang T, Xu JH, Zou Y, Chen R, Peng LR, Zhou ZD et al (2017b) Diffusion-weighted imaging (DWI) of hepatocellular carcinomas: a retrospective analysis of the correlation between qualitative and quantitative DWI and tumour grade. *Clin Radiol* 72(6):465–472
- Kan Z, Kobayashi S, Phongkitkarun S, Charnsangavej C (2005) Functional CT quantification of tumor perfusion after transhepatic arterial embolization in a rat model. *Radiology* 237(1):144–150
- Katsube T, Okada M, Kumano S, Hori M, Imaoka I, Ishii K et al (2011) Estimation of liver function using T1 mapping on Gd-EOB-DTPA-enhanced magnetic resonance imaging. *Investig Radiol* 46(4):277–283
- Khan K, Rata M, Cunningham D, Koh DM, Tunariu N, Hahne JC et al (2018) Functional imaging and circulating biomarkers of response to regorafenib in treatment-refractory metastatic colorectal cancer patients in a prospective phase II study. *Gut* 67(8):1484–1492
- Kim H, Booth CJ, Pinus AB, Chen P, Lee A, Qiu M et al (2008) Induced hepatic fibrosis in rats: hepatic steatosis, macromolecule content, perfusion parameters, and their correlations—preliminary MR imaging in rats. *Radiology* 247(3):696–705
- Kim SH, Kamaya A, Willmann JK (2014) CT perfusion of the liver: principles and applications in oncology. *Radiology* 272(2):322–344
- Kim JH, Joo I, Kim TY, Han SW, Kim YJ, Lee JM et al (2016) Diffusion-related MRI parameters for assessing early treatment response of liver metastases to cytotoxic therapy in colorectal Cancer. *AJR Am J Roentgenol* 207(3):W26–W32
- Kim YS, Jang YN, Song JS (2018) Comparison of gradient-recalled echo and spin-echo echo-planar imaging MR elastography in staging liver fibrosis: a meta-analysis. *Eur Radiol* 28(4):1709–1718
- Koh DM, Collins DJ (2007) Diffusion-weighted MRI in the body: applications and challenges in oncology. *AJR Am J Roentgenol* 188(6):1622–1635
- Koh DM, Collins DJ, Orton MR (2011) Intravoxel incoherent motion in body diffusion-weighted MRI: reality and challenges. *AJR Am J Roentgenol* 196(6):1351–1361

- Kokabi N, Ludwig JM, Camacho JC, Xing M, Mittal PK, Kim HS (2015) Baseline and early MR apparent diffusion coefficient quantification as a predictor of response of Unresectable hepatocellular carcinoma to doxorubicin drug-eluting bead chemoembolization. *JVIR* 26(12):1777–1786
- Lautt WW (1985) Mechanism and role of intrinsic regulation of hepatic arterial blood flow: hepatic arterial buffer response. *Am J Phys* 249(5 Pt 1):G549–G556
- Le Bihan D, Ichikawa S, Motosugi U (2017) Diffusion and Intravoxel incoherent motion MR imaging-based virtual Elastography: a hypothesis-generating study in the liver. *Radiology* 285(2):609–619
- Le Moigne F, Durieux M, Bancel B, Boublay N, Bousset L, Ducerf C et al (2012) Impact of diffusion-weighted MR imaging on the characterization of small hepatocellular carcinoma in the cirrhotic liver. *Magn Reson Imaging* 30(5):656–665
- Lee TY, Purdie TG, Stewart E (2003) CT imaging of angiogenesis. *Q J Nucl Med* 47(3):171–187
- Lee Y, Lee JM, Lee JE, Lee KB, Lee ES, Yoon JH et al (2014) MR elastography for noninvasive assessment of hepatic fibrosis: reproducibility of the examination and reproducibility and repeatability of the liver stiffness value measurement. *J Magn Reson Imaging* 39(2):326–331
- Leggett DA, Kelley BB, Bunce IH, Miles KA (1997) Colorectal cancer: diagnostic potential of CT measurements of hepatic perfusion and implications for contrast enhancement protocols. *Radiology* 205(3):716–720
- Liu Y, Matsui O (2007) Changes of intratumoral microvessels and blood perfusion during establishment of hepatic metastases in mice. *Radiology* 243(2):386–395
- Luo M, Zhang L, Jiang XH, Zhang WD (2017) Intravoxel incoherent motion diffusion-weighted imaging: evaluation of the differentiation of solid hepatic lesions. *Transl Oncol* 10(5):831–838
- Marquez HP, Puipe G, Mathew RP, Alkadhi H, Pfammatter T, Fischer MA (2017) CT perfusion for early response evaluation of radiofrequency ablation of focal liver lesions: first experience. *Cardiovasc Intervent Radiol* 40(1):90–98
- Materne R, Van Beers BE, Smith AM, Leconte I, Jamart J, Dehoux JP et al (2000) Non-invasive quantification of liver perfusion with dynamic computed tomography and a dual-input one-compartmental model. *Clin Sci (Lond)* 99(6):517–525
- Materne R, Smith AM, Peeters F, Dehoux JP, Keyeux A, Horsmans Y et al (2002) Assessment of hepatic perfusion parameters with dynamic MRI. *Magn Reson Med* 47(1):135–142
- Matsui O, Kobayashi S, Sanada J, Kouda W, Ryu Y, Kozaka K et al (2011) Hepatocellular nodules in liver cirrhosis: hemodynamic evaluation (angiography-assisted CT) with special reference to multi-step hepatocarcinogenesis. *Abdom Imaging* 36(3):264–272
- Miles KA, Hayball MP, Dixon AK (1993) Functional images of hepatic perfusion obtained with dynamic CT. *Radiology* 188(2):405–411
- Miles KA, Leggett DA, Kelley BB, Hayball MP, Sinnatamby R, Bunce I (1998) In vivo assessment of neovascularization of liver metastases using perfusion CT. *Br J Radiol* 71(843):276–281
- Miles KA, Lee TY, Goh V, Klotz E, Cuenod C, Bisdas S et al (2012) Current status and guidelines for the assessment of tumour vascular support with dynamic contrast-enhanced computed tomography. *Eur Radiol* 22(7):1430–1441
- Mule S, Pigneur F, Quelever R, Tenenhaus A, Baranes L, Richard P et al (2018) Can dual-energy CT replace perfusion CT for the functional evaluation of advanced hepatocellular carcinoma? *Eur Radiol* 28(5):1977–1985
- Murphy P, Hooker J, Ang B, Wolfson T, Gamst A, Bydder M et al (2015) Associations between histologic features of nonalcoholic fatty liver disease (NAFLD) and quantitative diffusion-weighted MRI measurements in adults. *J Magn Reson Imaging* 41(6):1629–1638
- Ng CS, Charnsangavej C, Wei W, Yao JC (2011) Perfusion CT findings in patients with metastatic carcinoid tumors undergoing bevacizumab and interferon therapy. *AJR Am J Roentgenol* 196(3):569–576
- Ng CS, Wei W, Duran C, Ghosh P, Anderson EF, Chandler AG et al (2018) CT perfusion in normal liver and liver metastases from neuroendocrine tumors treated with targeted antivascular agents. *Abdom Radiol (NY)* 43(7):1661–1669
- Ou HY, Bonekamp S, Bonekamp D, Corona-Villalobos CP, Torbenson MS, Geiger B et al (2013) MRI arterial enhancement fraction in hepatic fibrosis and cirrhosis. *AJR Am J Roentgenol* 201(4):W596–W602
- Padhani AR (2002) Dynamic contrast-enhanced MRI in clinical oncology: current status and future directions. *J Magn Reson Imaging* 16(4):407–422
- Padhani AR, Koh DM (2011) Diffusion MR imaging for monitoring of treatment response. *Magn Reson Imaging Clin N Am* 19(1):181–209
- Pan S, Wang XQ, Guo QY (2018) Quantitative assessment of hepatic fibrosis in chronic hepatitis B and C: T1 mapping on Gd-EOB-DTPA-enhanced liver magnetic resonance imaging. *World J Gastroenterol* 24(18):2024–2035
- Pandharipande PV, Krinsky GA, Rusinek H, Lee VS (2005) Perfusion imaging of the liver: current challenges and future goals. *Radiology* 234(3):661–673
- Park MJ, Kim YK, Lee MW, Lee WJ, Kim YS, Kim SH et al (2012) Small hepatocellular carcinomas: improved sensitivity by combining gadoteric acid-enhanced and diffusion-weighted MR imaging patterns. *Radiology* 264(3):761–770
- Patel J, Sigmund EE, Rusinek H, Oei M, Babb JS, Taouli B (2010) Diagnosis of cirrhosis with intravoxel incoherent motion diffusion MRI and dynamic contrast-enhanced MRI alone and in combination: preliminary experience. *J Magn Reson Imaging* 31(3):589–600
- Perumpail RB, Levitsky J, Wang Y, Lee VS, Karp J, Jin N et al (2012) MRI-guided biopsy to correlate tissue

- specimens with MR elastography stiffness readings in liver transplants. *Acad Radiol* 19(9):1121–1126
- Petitclerc L, Sebastiani G, Gilbert G, Cloutier G, Tang A (2017) Liver fibrosis: review of current imaging and MRI quantification techniques. *J Magn Reson Imaging* 45(5):1276–1295
- Petralia G, Fazio N, Bonello L, D'Andrea G, Radice D, Bellomi M (2011) Perfusion computed tomography in patients with hepatocellular carcinoma treated with thalidomide: initial experience. *J Comput Assist Tomogr* 35(2):195–201
- Reiner CS, Goetti R, Burger IA, Fischer MA, Frauenfelder T, Knuth A et al (2012) Liver perfusion imaging in patients with primary and metastatic liver malignancy: prospective comparison between ^{99m}Tc-MAA spect and dynamic CT perfusion. *Acad Radiol* 19(5):613–621
- Ren Y, Fleischmann D, Foygel K, Molvin L, Lutz AM, Koong AC et al (2012) Antiangiogenic and radiation therapy: early effects on in vivo computed tomography perfusion parameters in human colon cancer xenografts in mice. *Investig Radiol* 47(1):25–32
- Ronot M, Asselah T, Paradis V, Michoux N, Dorvillius M, Baron G et al (2010) Liver fibrosis in chronic hepatitis C virus infection: differentiating minimal from intermediate fibrosis with perfusion CT. *Radiology* 256(1):135–142
- Ronot M, Clift AK, Baum RP, Singh A, Kulkarni HR, Frilling A et al (2018) Morphological and functional imaging for detecting and assessing the Resectability of neuroendocrine liver metastases. *Neuroendocrinology* 106(1):74–88
- Rosenkrantz AB, Padhani AR, Chenevert TL, Koh DM, De Keyzer F, Taouli B et al (2015) Body diffusion kurtosis imaging: basic principles, applications, and considerations for clinical practice. *J Magn Reson Imaging* 42(5):1190–1202
- Sahani DV, Holalkere NS, Mueller PR, Zhu AX (2007) Advanced hepatocellular carcinoma: CT perfusion of liver and tumor tissue--initial experience. *Radiology* 243(3):736–743
- Sahani DV, Jiang T, Hayano K, Duda DG, Catalano OA, Ancukiewicz M et al (2013) Magnetic resonance imaging biomarkers in hepatocellular carcinoma: association with response and circulating biomarkers after sunitinib therapy. *J Hematol Oncol* 6:51
- Schuppan D, Afdhal NH (2008) Liver cirrhosis. *Lancet* 371(9615):838–851
- Serai SD, Yin M, Wang H, Ehman RL, Podberesky DJ (2015) Cross-vendor validation of liver magnetic resonance elastography. *Abdom Imaging* 40(4):789–794
- Serai SD, Obuchowski NA, Venkatesh SK, Sirlin CB, Miller FH, Ashton E et al (2017) Repeatability of MR Elastography of liver: a meta-analysis. *Radiology* 285(1):92–100
- Shao S, Shan Q, Zheng N, Wang B, Wang J (2019) Role of Intravoxel incoherent motion in discriminating hepatitis B virus-related intrahepatic mass-forming Cholangiocarcinoma from hepatocellular carcinoma based on liver imaging reporting and data system v2018. *Cancer Biother Radiopharm*
- Shire NJ, Yin M, Chen J, Raikar RA, Fox-Bosetti S, Johnson SM et al (2011) Test-retest repeatability of MR elastography for noninvasive liver fibrosis assessment in hepatitis C. *J Magn Reson Imaging* 34(4):947–955
- Singh S, Venkatesh SK, Wang Z, Miller FH, Motosugi U, Low RN et al (2015) Diagnostic performance of magnetic resonance elastography in staging liver fibrosis: a systematic review and meta-analysis of individual participant data. *Clin Gastroenterol Hepatol* 13(3):440–51 e6
- Sourbron S (2010) Technical aspects of MR perfusion. *Eur J Radiol* 76(3):304–313
- Sourbron S, Sommer WH, Reiser MF, Zech CJ (2012) Combined quantification of liver perfusion and function with dynamic gadoteric acid-enhanced MR imaging. *Radiology* 263(3):874–883
- Stewart EE, Chen X, Hadway J, Lee TY (2008) Hepatic perfusion in a tumor model using DCE-CT: an accuracy and precision study. *Phys Med Biol* 53(16):4249–4267
- Taouli B, Koh DM (2010) Diffusion-weighted MR imaging of the liver. *Radiology* 254(1):47–66
- Thng CH, Koh TS, Collins D, Koh DM (2014) Perfusion imaging in liver MRI. *Magn Reson Imaging Clin N Am* 22(3):417–432
- Tofts PS (1997) Modeling tracer kinetics in dynamic Gd-DTPA MR imaging. *J Magn Reson Imaging* 7(1):91–101
- Tsushima Y, Blomley JK, Kusano S, Endo K (1999) The portal component of hepatic perfusion measured by dynamic CT: an indicator of hepatic parenchymal damage. *Dig Dis Sci* 44(8):1632–1638
- Tsushima Y, Blomley MJ, Yokoyama H, Kusano S, Endo K (2001) Does the presence of distant and local malignancy alter parenchymal perfusion in apparently disease-free areas of the liver? *Dig Dis Sci* 46(10):2113–2119
- Van Beers BE, Leconte I, Materne R, Smith AM, Jamarat J, Horsmans Y (2001) Hepatic perfusion parameters in chronic liver disease: dynamic CT measurements correlated with disease severity. *AJR Am J Roentgenol* 176(3):667–673
- Venkatesh SK, Yin M, Glockner JF, Takahashi N, Araoz PA, Talwalkar JA et al (2008) MR elastography of liver tumors: preliminary results. *AJR Am J Roentgenol* 190(6):1534–1540
- Vilgrain V, Esvan M, Ronot M, Caumont-Prim A, Aube C, Chatellier G (2016) A meta-analysis of diffusion-weighted and gadoteric acid-enhanced MR imaging for the detection of liver metastases. *Eur Radiol* 26(12):4595–4615
- Wang XM, Zhang XJ, Ma L (2018) Diagnostic performance of magnetic resonance technology in detecting steatosis or fibrosis in patients with nonalcoholic fatty liver disease: a meta-analysis. *Medicine (Baltimore)* 97(21):e10605

- Watanabe H, Kanematsu M, Goshima S, Kondo H, Onozuka M, Moriyama N et al (2011) Staging hepatic fibrosis: comparison of gadoxetate disodium-enhanced and diffusion-weighted MR imaging--preliminary observations. *Radiology* 259(1):142–150
- Winfield JM, Tunariu N, Rata M, Miyazaki K, Jerome NP, Germuska M et al (2017) Extracranial soft-tissue tumors: repeatability of apparent diffusion coefficient estimates from diffusion-weighted MR imaging. *Radiology* 284(1):88–99
- Wu H, Liang Y, Jiang X, Wei X, Liu Y, Liu W et al (2018) Meta-analysis of intravoxel incoherent motion magnetic resonance imaging in differentiating focal lesions of the liver. *Medicine (Baltimore)* 97(34):e12071
- Yang L, Zhang XM, Tan BX, Liu M, Dong GL, Zhai ZH (2012) Computed tomographic perfusion imaging for the therapeutic response of chemoembolization for hepatocellular carcinoma. *J Comput Assist Tomogr* 36(2):226–230
- Yang L, Rao S, Wang W, Chen C, Ding Y, Yang C et al (2018) Staging liver fibrosis with DWI: is there an added value for diffusion kurtosis imaging? *Eur Radiol* 28(7):3041–3049
- Yankeelov TE, Gore JC (2009) Dynamic contrast enhanced magnetic resonance imaging in oncology: theory, data acquisition, analysis, and examples. *Curr Med Imaging Rev* 3(2):91–107
- Yin M, Talwalkar JA, Glaser KJ, Manduca A, Grimm RC, Rossman PJ et al (2007) Assessment of hepatic fibrosis with magnetic resonance elastography. *Clin Gastroenterol Hepatol* 5(10):1207–13 e2
- Yoon JH, Lee JM, Baek JH, Shin CI, Kiefer B, Han JK et al (2014) Evaluation of hepatic fibrosis using intravoxel incoherent motion in diffusion-weighted liver MRI. *J Comput Assist Tomogr* 38(1):110–116
- Yoon JH, Lee JM, Paek M, Han JK, Choi BI (2016) Quantitative assessment of hepatic function: modified look-locker inversion recovery (MOLLI) sequence for T1 mapping on Gd-EOB-DTPA-enhanced liver MR imaging. *Eur Radiol* 26(6):1775–1782
- Yoon JH, Lee JM, Kim E, Okuaki T, Han JK (2017) Quantitative liver function analysis: volumetric T1 mapping with fast multisection B1 inhomogeneity correction in hepatocyte-specific contrast-enhanced liver MR imaging. *Radiology* 282(2):408–417
- Yoon JH, Lee JM, Kang HJ, Ahn SJ, Yang H, Kim E et al (2019) Quantitative assessment of liver function by using Gadoteric acid-enhanced MRI: hepatocyte uptake ratio. *Radiology* 290(1):125–133